Archives of Biochemistry and Biophysics 573 (2015) 59–68

Contents lists available at ScienceDirect

Archives of Biochemistry and Biophysics

journal homepage: www.elsevier.com/locate/yabbi

Altering the substrate specificity of methyl parathion hydrolase with directed evolution

Tee-Kheang Ng [a], Lawrence R. Gahan [b], Gerhard Schenk [b], David L. Ollis [a,*]

[a] Research School of Chemistry, Australian National University, Canberra, ACT 0200, Australia
[b] School of Chemistry and Molecular Biosciences, The University of Queensland, St Lucia, Brisbane, QLD 4072, Australia

ARTICLE INFO

Article history:
Received 2 December 2014
and in revised form 10 March 2015
Available online 19 March 2015

Keywords:
Organophosphate pesticides
Bioremediation
Methyl parathion hydrolase
Substrate specificity
Directed evolution

ABSTRACT

Many organophosphates (OPs) are used as pesticides in agriculture. They pose a severe health hazard due to their inhibitory effect on acetylcholinesterase. Therefore, detoxification of water and soil contaminated by OPs is important. Metalloenzymes such as methyl parathion hydrolase (MPH) from *Pseudomonas* sp. WBC-3 hold great promise as bioremediators as they are able to hydrolyze a wide range of OPs. MPH is highly efficient towards methyl parathion ($1 \times 10^6\ s^{-1}\ M^{-1}$), but its activity towards other OPs is more modest. Thus, site saturation mutagenesis (SSM) and DNA shuffling were performed to find mutants with improved activities on ethyl paraxon ($6.1 \times 10^3\ s^{-1}\ M^{-1}$). SSM was performed on nine residues lining the active site. Several mutants with modest activity enhancement towards ethyl paraoxon were isolated and used as templates for DNA shuffling. Ultimately, 14 multiple-site mutants with enhanced activity were isolated. One mutant, R2F3, exhibited a nearly 100-fold increase in the k_{cat}/K_m value for ethyl paraoxon ($5.9 \times 10^5\ s^{-1}\ M^{-1}$). These studies highlight the 'plasticity' of the MPH active site that facilitates the fine-tuning of its active site towards specific substrates with only minor changes required. MPH is thus an ideal candidate for the development of an enzyme-based bioremediation system.

Introduction

Organophosphates (OPs)[1] constitute the most commonly used pesticides in agriculture and account for approximately 40% of total pesticide usage [1]. OP are generally toxic as they inhibit acetylcholinesterase, a serine hydrolase that catalyzes the breakdown of acetylcholine at cholinergic synapses, leading to hyperstimulation of nerve cells and death [2]. It is estimated that OPs are responsible for up to 3,000,000 poisonings and 220,000 deaths annually [3]. Oximes, a group of strong nucleophiles, were shown to be capable to reactivate inhibited acetylcholinesterase [4,5], and current treatments for OP poisoning rely on chemical antidotes such as cholinolytics, oximes, atropine and anticonvulsants to minimize toxic manifestations [6]. However, these antidotes have to be administered soon after exposure, as they are impotent against aged inhibited acetylcholinesterase. Furthermore, the effectiveness of oxime reactivation appears to depend on the identity of the OP compounds [7]. Excess OPs in the bloodstream will also re-inhibit acetylcholinesterase if they are not removed. Therefore, there is an urgent need to develop (i) methods to remove OPs from contaminated soils, as well as (ii) therapies to treat OP poisoning and (iii) biosensors for OP detection.

The use of OP-degrading enzymes is an effective approach for OP decontamination. Methyl parathion hydrolase (MPH; E.C. 3.1.8.1), a metal ion-dependent enzyme isolated from *Pseudomonas* sp. WBC-3, has attracted considerable attention due to its ability to hydrolyze a broad range of OPs [8,9]. The crystal structure of MPH reveals an αββα fold, characteristic for metallohydrolases [10]. Interestingly, MPH is structurally similar to metallo-β-lactamases (MBLs) from the B3 subgroup, including the enzyme L1 from *Stenotrophomonas maltophilia* and AIM-1 from *Pseudomonas aeruginosa*. MBLs are Zn^{2+}-dependent enzymes that have emerged as major threat to global health since they are capable of inactivating most of the commonly used antibiotics [11,12].

MPH is able to hydrolyze methyl parathion (MPS) at a rapid rate, with a k_{cat}/K_m ratio of $>10^6\ M^{-1}\ s^{-1}$ [10]. Limited information about the substrate preference and reaction mechanism of MPH is currently available. Residues Leu65, Leu67, Phe119, Trp179,

* Corresponding author.
E-mail address: ollis@rsc.anu.edu.au (D.L. Ollis).

[1] *Abbreviations used:* OP, organophosphate; MPH, methyl parathion hydrolase; SSM, site saturation mutagenesis; MBls, metallo-β-lactamases; EPO, ethyl paraoxon; LB, Luria–Bertani; StEP, staggered extension process; MCO, methyl chlorpyrifos oxon; ECO, ethyl chlorpyrifos oxon; TCPy, 3,5,6-trichloro-2-pyridinol.

http://dx.doi.org/10.1016/j.abb.2015.03.012
0003-9861/

Phe196, Leu258 and Leu273 are part of the substrate binding pocket [10]; while the substitutions of Phe196 and Leu273 by alanines enhanced enzymatic activity towards the substrate *p*-nitrophenyl diphenylphosphate [13], replacing Phe119, Trp179 and Phe196 by alanines is detrimental for the catalytic activity towards MPS [10].

An ideal bioremediator exhibits significant levels of activity for a broad range of OPs. Considering the close structural similarity between MPH and enzymes from the MBL superfamily, we hypothesized that the substrate specificity of MPH can be altered easily. Here, site saturation mutagenesis (SSM) was performed to generate mutant libraries that were screened for improved activity towards ethyl paraoxon (EPO), a substrate that is approximately 100-fold less efficient than MPS in the wild-type enzyme. Mutants isolated from each library were used as parents for DNA shuffling to obtain further enhancement towards EPO. Several mutants with significant improvement also towards "poor" substrates (*e.g.* chlorpyrifos) were thus found. The results highlight the active site 'plasticity' of MPH and establish this enzyme as a promising agent to be employed in bioremediation applications.

Materials and methods

Materials, bacterial strains, growth conditions and plasmids

Pesticides were purchased from either Chem Service (West Chester, PA, USA) or Sigma Aldrich (St. Louis, MO, USA). Molecular biology reagents and enzymes were obtained from New England Biolabs (Ipswich, MA, USA), Thermo Scientific (Waltham, MA, USA) or Sigma–Aldrich (St. Louis, MO, USA). DNA primers (Table S1 in Supplemental material) were synthesized by Geneworks (Hindmarsh, SA, Australia) or Integrated DNA Technologies (Coralville, IA, USA). Plasmid extraction and purification kits were obtained from Qiagen (Limburg, Netherlands) or Promega (Madison, WI, USA). Protein purification columns were purchased from GE Healthcare (Buckinghamshire, UK). *Escherichia coli* strain DH5α was used for all aspects of the work described. Cells harboring pJWL1030 plasmids were grown at 37 °C on Luria–Bertani (LB) broth or agar plates supplemented with 50 μg/mL kanamycin. Construction of pJWL1030 plasmid has been described previously [14]. *mpd*, the gene coding for MPH, was synthesized by DNA 2.0 (Menlo Park, CA, USA). The recombinant plasmid containing the *mpd* gene (MPH-pJWL1030) was constructed by amplification from the MPH-pET47b plasmid using primers P1 and P2. The nucleotides that encode the first 35 amino acid residues that constitute the signal peptide were excluded in this amplification. The PCR product was digested with *Ase*I and *Pst*I, and ligated into the *Nde*I and *Pst*I sites, and transformed into *E. coli* DH5α using electroporation.

Structural superimposition studies

The superimposition of MPH with MBL superfamily enzymes was done in two stages in PyMOL. PyMOL's Cealign command was initially used for the superimpositions. Minor adjustments were then added using PyMOL's pair fitting function, by using the two active site metals, the bridging water and metal coordination residues of MPH and a target protein as points of alignment. The PDB IDs used in the superimposition study were 1P9E [10], 4AWY [15], 1BVT [16], 1X8G [17], 1SML [18], 1QH5 [19], 2QED [20], 2BR6 [21] and 2CBN [22].

Library generation

The SSM libraries were constructed using a megaprimed, ligase-free site specific mutagenesis method reported by Tseng et al. [23] and Sanchis et al. [24]. The PCR reactions were performed using 30 ng of template DNA (WTMPH-pJWL1030), 1× HF buffer, 1.5 mM $MgCl_2$, 0.1 μM of each mutagenic and flanking primer, 1 U of Phusion polymerase (Thermo Scientific, Waltham, MA, USA) and 0.2 mM of each dNTP. The amplification program for mutagenesis was as follows: initial denaturation for 3 min at 98 °C, followed by 18 cycles of 1 min at 98 °C, annealing for 1 min at 55 °C and extension at 72 °C. The second stage consisted of 25 cycles of 1 min at 98 °C and extension for 5 min at 68 °C and a final extension for 10 min at 68 °C. Up to four reactions were pooled and treated with 20 U of *Dpn*I twice at 37 °C for 1 h each. The PCR product was subsequently purified and 2 μL of the product was transformed into *E. coli* DH5α using electroporation. Primers P2 and P3 were used to generate the L67P68R72-NDT library; P2 and P4 to generate the R72-NNK library; P2 and P5 to generate the F119-NDT library; P2 and P6 to generate the P150-NDT library; P2 and P7 to generate the W179-NNK library; P1 and P8 to generate the F196-NDT library; P1 and P9 to generate the L258-NDT library and P1 and P10 to generate the L273-NDT library. The sequences of the primers are shown in Table S1. NDT (N = A, C, G or T; D = A, G or T) randomisation was used in all libraries except R72-NNK and W179-NNK.

Shuffling of mutations isolated from the SSM library was performed using the staggered extension process (StEP) [25]. The StEP reaction (25 μL) was performed in a solution containing 30 ng of template DNA, 1 μM of the P1 and P2 primers, 0.2 mM of each dNTP, 1× HF buffer and 1 U of Phusion polymerase. The amplification program for StEP was as follows: initial denaturation for 5 min at 98 °C, followed by 120 cycles for 10 s at 98 °C, annealing for 10 s at 55 °C, extension for 2 s at 72 °C, final annealing for 2 min at 55 °C and final extension for 5 min at 72 °C. Up to four reactions were pooled, purified and digested with *Ase*I and *Pst*I. The digested PCR product was cloned into pJWL1030 as described for the construction of MPH-pJWL1030.

Library screening

The library screening procedures consisted of a primary and secondary screen. The primary screen master plate was prepared either by picking single colonies that were then inoculated in 96-well plates or by culture dilution methods developed by Stevenson et al. [26]. The former was used for most of the generated SSM and StEP shuffling libraries, while the latter was used for the L67P68R72-NDT library due to its much larger size. Mutants were subsequently transformed into *E. coli* DH5α; single colonies were picked and inoculated in 96-well round-bottomed plates (Sarstedt, Nümbrecht, Germany) containing 100 μL LB broth supplemented with 0.1 mM $ZnCl_2$ and 50 μg/mL kanamycin. For the culture dilution method, the transformants were diluted with LB-kanamycin supplemented with 0.1 mM $ZnCl_2$ and dispensed into 96-well round-bottom plates at as density of 3–4 cells per 100 μL. The plates were incubated for 24 h at 37 °C. Prior to activity assays, the cultures were resuspended by gentle pipetting and 10 μL of the 100 μL culture from each well was aliquoted into 96-well flat-bottom plates (Sarstedt, Nümbrecht, Germany) and lyzed with 10 μL of 0.5× BugBuster (Novagen, Darmstadt, Germany) for 15 min. The lysate was assayed with 119 μM ethyl paraoxon (EPO) in 50 mM HEPES, 100 mM NaCl, 0.1 mM $ZnCl_2$, pH 7.6, in a final volume of 200 μL. The activity was monitored by the release of *p*-nitrophenolate at 405 nm using a Spectramax M2e Microplate reader (Molecular devices, Sunnyvale, CA, USA) at 30 °C. The assay procedure was adapted and modified from reference [27]. Mutants that showed improved EPO activity were streaked on fresh LB-kanamycin plates and single colonies were picked for a secondary screen. The secondary screen assay was performed exactly as described for the primary screen. For the culture

dilution primary screen method, up to five single colonies were picked from the streaking of each chosen well for the secondary screen. Improved mutants were streaked on fresh LB-kanamycin plates and single colonies were picked and grown for plasmid isolation and DNA sequencing.

Expression and purification

All MPH variants were expressed constitutively in the pJWL1030 vector. A starter culture consisting of 300 μL LB-kanamycin broth supplemented with 0.1 mM $ZnCl_2$ was inoculated with single colonies of cells harboring the MPH-pJWL1030 plasmid and grown at 37 °C for 16 h. The starter culture was then inoculated onto 30 mL LB-kanamycin broth, supplemented with 0.1 mM $ZnCl_2$ and was grown at 37 °C for 24 h. The cells were harvested by centrifugation and were kept at −80 °C until use.

All purification steps were carried out at 4 °C. The harvested cells were resuspended in 10 mL, 20 mM HEPES, pH 7.0, 0.1 mM $ZnCl_2$, 1 mM phenylmethylsulfonyl fluoride, and were disrupted with a French Press (12,000 psi cell pressure, two repeats). The cell debris was removed by centrifugation and the soluble fraction was loaded onto a 5 mL SP Sepharose Fast Flow column that has been equilibrated with 20 mM HEPES, pH 7.0, 0.1 mM $ZnCl_2$. The bound protein was eluted with a linear 0–1 M NaCl gradient in the same buffer. SDS–PAGE analysis of the eluted MPH showed >90% purity. For storage MPH was dialyzed against 50 mM HEPES, pH 7.6, 100 mM NaCl, 0.1 mM $ZnCl_2$. 50% (v/v) glycerol was included as cryoprotectant for storage at −20 °C. The concentration of MPH was determined by measuring A_{280}. The extinction coefficients (ε_{280}) were estimated using the ProtParam tool (http://web.expasy.org/protparam/); for most variants ε_{280} is 20,400 M^{-1} cm^{-1}, except for the F119Y, F196Y, R1A6, R2D2, R2A2, R2F3 and R2D3 mutants, where ε_{280} is estimated to be 21,800 M^{-1} cm^{-1}.

Kinetic studies

The kinetic constants of wild-type MPH and its mutants were obtained by varying the concentrations of six substrates in 50 mM HEPES, pH 7.6, 100 mM NaCl, 0.1 mM $ZnCl_2$. The assays were performed in either a 96-well flat-bottomed plate (200 μL reaction volume), or a in micro-cuvette (1 mL). The 96-well plate assays were monitored with a Spectramax M2e Microplate reader and a Cary 1E UV–Vis spectrophotometer was used for the micro-cuvette assays. The assayed substrates (and concentration ranges used) were methyl parathion (MPS; 7.6–189.9 μM), methyl paraoxon (MPO; 15.2–379.8 μM), ethyl parathion (EPS; 15.2–60.8 μM), ethyl paraoxon (EPO; 15.2–379.8 μM), methyl chlorpyrifos oxon (MCO; 30.4–379.8 μM) and ethyl chlorpyrifos oxon (ECO; 30.4–379.8 μM). The hydrolyses of MPS, MPO, EPS, EPO were monitored via the release of the *p*-nitrophenolate product at 405 nm (ε_{405} = 14,696.56 M^{-1} cm^{-1} at pH 7.6), while the hydrolyses of MCO and ECO were monitored via the release of the 3,5,6-trichloro-2-pyridinol product at 310 nm (ε_{310} = 5800.67 M^{-1} cm^{-1} at pH 7.6) using a Cary 1E UV–Vis spectrophotometer (Varian, Palo Alto, CA, USA). All kinetic measurements were done in a final volume of 1 mL at 30 °C. The kinetics constants were determined by fitting the data to the Michaelis–Menten equation (Eq. (1)) using KaleidaGraph 4.1 software (Synergy, Reading, PA, USA):

$$v_o = V_{max}S/(K_m + S) \quad (1)$$

where v_o is the initial velocity, V_{max} (=$k_{cat}[E]$) is the maximum velocity, S is the substrate concentration and K_m is the Michaelis constant. The error represents the standard deviation from three independent experiments.

Homology modelling and substrate docking

SWISS-MODEL [28–30] was used to generate models of the structures of MPH mutants isolated in the evolution experiments. Subunit B of wild-type MPH (PDB ID: 1P9E_b) was used as the template for the modelling. AutoDock Vina [31] and Swiss-Dock [32,33] were used to perform molecular docking of the substrate MPS into the active site of subunit B of MPH. The structure of MPS was obtained from the ZINC database (http://zinc.docking.org/; ZINC ID: 02040890).

Results and discussion

Assessing the substrate profile of wild-type MPH

In order to assess the substrate preference of wild-type MPH, specific activities towards various substrates were measured (Fig. 1). The structures of the substrates used are illustrated in Fig. 2. Of the various OPs investigated, MPH shows a distinct preference towards dimethyl-substituted substrates such as methyl parathion (MPS), methyl paraoxon (MPO) and methyl chlorpyrifos oxon (MCO), when compared to diethyl-substituted analogues such as ethyl parathion (EPS), ethyl paraoxon (EPO) or ethyl chlorpyrifos oxon (ECO). The enzyme also prefers substrates containing the 3,5,6-trichloro-2-pyridinol (TCPy) rather than the *p*-nitrophenol (pNP) leaving group. MPH has no detectable activity towards the monoester *p*-nitrophenyl phosphate and diester bis-(*p*-nitrophenyl) phosphate, and only very low activity towards the carboxylester *p*-nitrophenyl acetate. EPO, which is turned over ~100-fold slower than MPS, was chosen as the substrate for library screening. EPO possesses two features that are common among poor substrates of MPH – it has a diethyl substituent and a phosphoryl group (P═O). The reason for the preference of MPH for thionates (thiophosphoryl containing OPs) is unknown but is unique among phosphotriesterases [34].

Site saturation mutagenesis and DNA shuffling

MPH is part of the MBL superfamily that covers a diverse range of catalytic functions. Seven structures from that group were obtained from the Protein Data Bank (http://www.rcsb.org/pdb/home/home.do) and superimposed onto subunit B of MPH to select the residues to mutate. The metal ions and metal ion binding ligands in the binuclear active sites superimpose generally with good agreement. It is also noted that the MPH active site is the most crowded of all the structures compared – all the other active sites are more open than that of MPH. This difference is illustrated in Fig. 3, in which MPH is displayed in cartoon mode with side

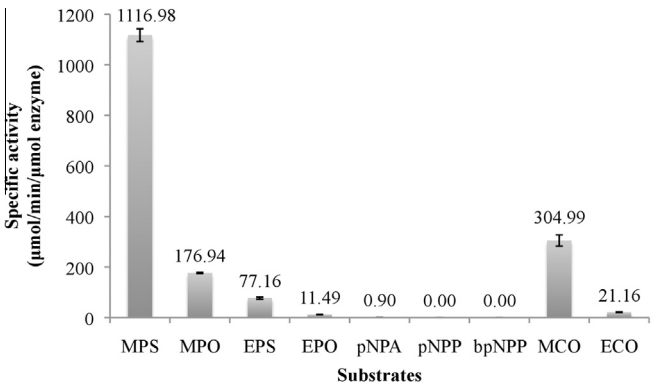

Fig. 1. Catalytic activity of wild-type MPH towards various substrates.

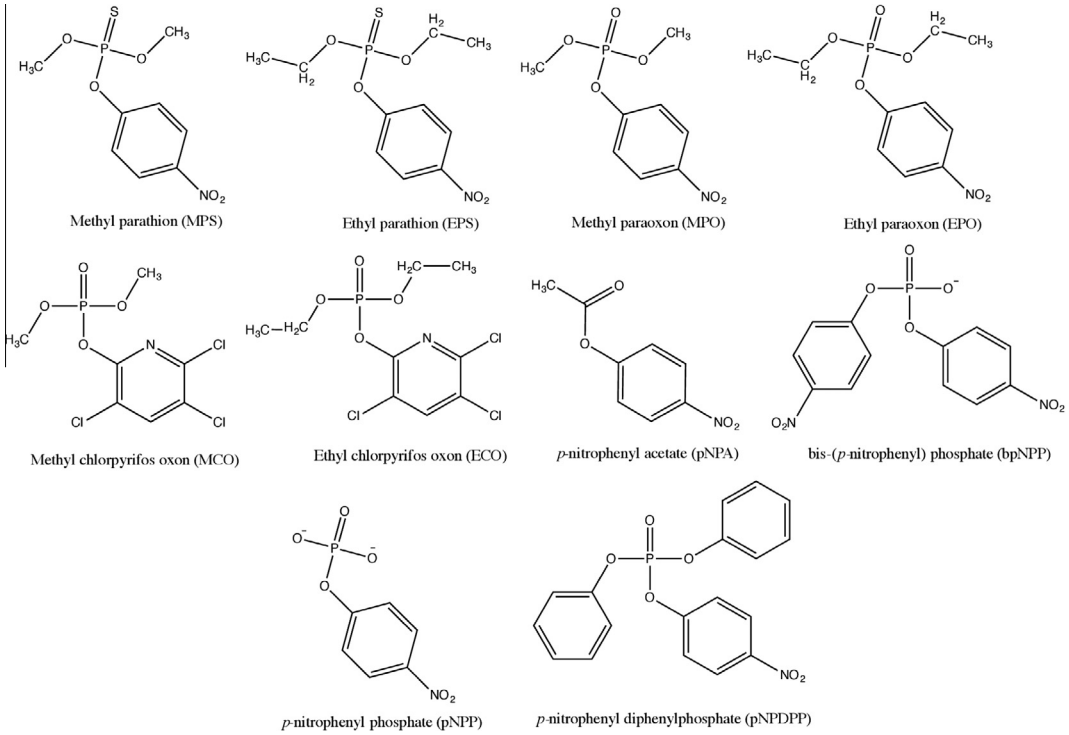

Fig. 2. Structures of organophosphate substrates used in this work.

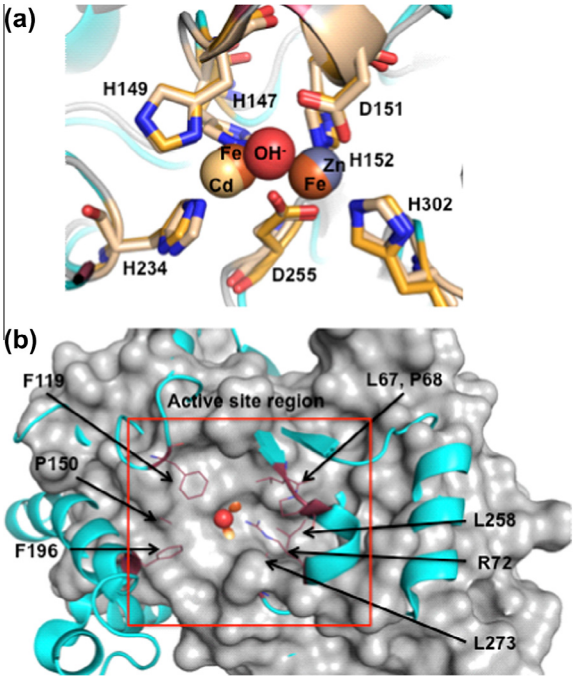

Fig. 3. (a) Structural superimposition of the metal ion ligands of MPH and GloB. The amino acid numbering scheme from MPH was used in labelling the metal ion-binding ligands. The MPH ligands are colored yellow while GloB ligands are colored in white. (b) GloB is shown in surface representation mode and MPH in cyan. MPH residues that line the active site and are different from those in GloB are colored in maroon. (For interpretation of the references to color in this figure legend, the reader is referred to the web version of this article.)

chains displayed in lines, while *Salmonella typhimurium* GloB (PDB ID: 2QED), a glyoxalase II, is displayed in surface representation mode. It is evident that the major portion of the MPH active site overlaps with that of the representative MBL member, suggesting that the relevant amino acid residues fulfil a structural role and are not important for discriminating between substrates. Thus, the residues in the MPH active site that do not overlap with residues of GloB may be important for determining the substrate specificity of MPH. These residues are L67, P68, R72, F119, P150, F196, L258 and L273. W179 was also selected since it was previously suggested as a residue involved in substrate binding [10]. The location of these residues in the structure is shown in Fig. 4.

Eight SSM libraries were generated and screened for mutants that showed improved activity towards EPO (Table 1). NDT (N = A, C, G or T; D = A, G or T) randomization was used in most libraries to produce small and efficient libraries, an approach that was particularly useful for the L67P68/R72-NDT library, where three residues were simultaneously mutated [35]. NDT produces a balanced mix of polar and non-polar, aliphatic and aromatic, as well as negatively and positively charged representatives, while excluding most of the structurally similar amino acids through 12 codon combinations that encode 12 amino acids without

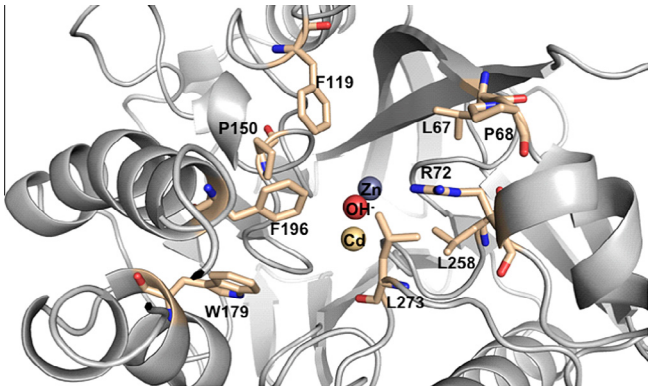

Fig. 4. Location of the MPH residues selected for site saturation mutagenesis.

Table 1
Summary of site saturation libraries generated, randomization used and the number of mutants screened. The number of possible variants and oversampling required for 95% coverage was calculated using CASTer 2.0.

SSM library	Codon randomisation	Number of possible variants	Library size to achieve 95% coverage	Number of mutants screened	Beneficial mutations	Detrimental mutations
L67P68R72	NDT–NDT–NDT	1278	5175	5800	None	Did not sample
R72	NNK	32	94	80	None	A, T, G
F119	NDT	12	34	40	Y	G, N
P150	NDT	12	34	40	None	Y, H, G
W179	NNK	32	94	80	None	S, H, Y, M
F196	NDT	12	34	40	I, L, Y	R, D
L258	NDT	12	34	40	I, S, N, H	R
L273	NDT	12	34	40	I, V	C, D

redundancy [35]. A small number of mutants with diminished activity was also sampled randomly from each library to examine the mutations that caused the decrease in activity. Overall, only mutations affecting F119, F196, L258 and L273 resulted in enhanced activity.

A quick relative activity validation test was carried out on mutants that showed improvement towards EPO hydrolysis during screening in order to establish a shortlist of promising mutants for more detailed kinetic studies (data not shown). Ten mutants, namely F119Y, F196L, F196I, F196Y, L258S, L258I, L258H, L258N, L273I and L273V, were thus picked for protein expression, purification and kinetic studies. Further activity enhancement (via shuffling) was deemed possible as each of the single site mutants has enhanced activity against EPO. Together with wild-type MPH these mutants were thus employed as parents in further shuffling experiments using the staggered extension process (StEP) approach [36]. The resulting mutants were subsequently tested for further enhancement in EPO activity. Two rounds of StEP shuffling were carried out, with multiple site variants isolated from the first round being used as parents in the second; the results or these screens are summarized in Table 2. After two rounds of StEP, only double- and triple-site mutants were isolated, possibly due to the distance between some of the mutations. For example, L258 and L273 are separated by only 45 nucleotides. The recombination efficiency decreases as the distance between mutations decreases [36].

Kinetic analysis of MPH variants

Each of the single site variants with improved hydrolytic activity towards EPO was expressed, purified and its catalytic properties were investigated with six OP substrates (other than EPO, which was used in library screening) to probe possible additional alterations to the substrate preference of MPH. For multiple site variants the crude lysate was used in initial screens to pre-select the mutants of interest. R1A6, R2B2, R2C2, R2D2, R2A2, R2F3 and R2D4 were thus selected for purification and detailed kinetic studies. Mutants that were not selected either have only moderate catalytic improvement, or are represented by other mutants that exhibit similar catalytic properties. The kinetics parameters for the various MPH variants are summarized in Table 3.

Table 2
Summary of StEP libraries generated, number of mutants screened and improved mutants selected from the screen.

StEP	Number of mutants screened	Selected mutants	Residue			
			F119	F196	L258	L273
Round 1	400	R1B2	Y		N	
		R1D4		I		V
		R1A6	Y		S	
		R1B6		I	N	
		R2B2		I	H	
		R2C2		I		I
		R2D2	Y		H	
		R2F2		Y	H	
Round 2	400	R2G4		L	H	
		R2A2	Y	I		V
		R2E3	Y	I	N	
		R2F3	Y	I	H	
		R2C4	Y	Y	H	
		R2D4	Y	I		I

In general, each of the single site mutants selected from the EPO screen displays modest enhancement in k_{cat}/K_m towards that substrate, with the best single site mutant, L258H, having a sevenfold improvement. Furthermore, apart from L258I, they have decreased k_{cat}/K_m ratios towards MPS, the preferred substrate for wild-type MPH. Each of the multiple site variants displays further improvements towards EPO hydrolysis in terms of both k_{cat} and k_{cat}/K_m. The most efficient mutant, R2F3, has a nearly 100-fold improvement in the k_{cat}/K_m ratio towards EPO. Each of the multiple site variants also recorded improved efficiency towards ECO (in contrast to the single site variants, where only a subset displayed an increase). Most of the multiple site mutants have, however, a lower k_{cat} and k_{cat}/K_m towards MPS and EPS, indicating a shift in substrate specificity away from substrates with the P═S group. The catalytic parameters of L258S, L258H, R2B2, R2C2, R2F3 and R2D4 for the EPS hydrolysis were not determined due to their low activity.

F119 and F196 – aromatic residues are required for high activity

F119 appears to be more important than F196 for MPH activity. The activity distribution profiles of F119 and F196 libraries show different mutational tolerances (Fig. S1 in the Supplemental material); over 70% of the F119 library but less than 50% of the F196 library display an activity towards EPO that is at least half as high as that of wild-type MPH. F119Y is the only mutant with improved reactivity towards EPO from the F119 library, while F196L, F196I and F196Y from the F196 library all have improved reactivity, suggesting that an aromatic ring in position 119, but not in position 196 is necessary for efficient catalysis. This hypothesis is further supported by a comparison of the active sites of MPH and OPHC2 from *Pseudomonas pseudoalcaligenes.* OPCH2 is a promiscuous hydrolase that shares near identical protein structure with MPH despite only 48% amino acid sequence similarity (Fig. S2 in the Supplemental material) [37]. In OPHC2 (PDB ID: 4LE6), the residue equivalent to F196 is replaced by a methionine (M188), while F119 is conserved (F111). Thus, F119 may play an important role in substrate binding, possibly via the formation of π–stacking interactions with the aromatic ring of OP substrates.

L258 – flexible position that is key to altering MPH specificity

L258 is of particular interest as four different mutations were found to lead to significantly improved activity towards EPO.

Table 3
Catalytic parameters for (A) single-site MPH mutants and (B) multiple-site MPH mutants. The errors for k_{cat}, K_m and k_{cat}/K_m represent the standard deviation of three independent experiments. ND: Not determined.

A

OPs	Variant	k_{cat} (s^{-1})	Relative k_{cat}	K_m (μM)	Relative K_m	k_{cat}/K_m (s^{-1} mM^{-1})	Relative k_{cat}/K_m
MPS	**WT**	27.5 ± 0.2	1.0	27.3 ± 1.4	1.0	1010 ± 50	1.0
	F119Y	28.9 ± 2.4	1.1	30.1 ± 1.0	1.1	970 ± 120	1.0
	F196L	1.5 ± 0.2	0.1	52.2 ± 9.8	1.9	29 ± 2	0.0
	F196I	1.7 ± 0.1	0.1	13.9 ± 2.6	0.5	130 ± 20	0.1
	F196Y	34.5 ± 1.5	1.3	37.8 ± 2.8	1.4	910 ± 30	0.9
	L258S	1.2 ± 0.1	0.0	26.0 ± 5.1	1.0	47 ± 5	0.0
	L258I	14.4 ± 0.5	0.5	5.9 ± 0.8	0.2	2480 ± 250	2.5
	L258H	1.7 ± 0.1	0.1	17.0 ± 3.0	0.6	100 ± 10	0.1
	L258N	3.5 ± 0.2	0.1	49.3 ± 10.9	1.8	70 ± 10	0.1
	L273I	3.0 ± 0.2	0.1	12.9 ± 3.1	0.5	240 ± 40	0.2
	L273V	7.7 ± 0.5	0.3	9.2 ± 1.2	0.3	840 ± 70	0.8
MPO	**WT**	4.5 ± 0.2	1.0	72.8 ± 6.7	1.0	62 ± 3	1.0
	F119Y	8.7 ± 0.9	1.9	244.4 ± 33.9	3.4	36 ± 2	0.6
	F196L	1.1 ± 0.1	0.2	298.5 ± 28.3	4.1	4 ± 0	0.1
	F196I	1.3 ± 0.2	0.3	290.0 ± 46.7	4.0	5 ± 0	0.1
	F196Y	5.9 ± 0.4	1.3	181.8 ± 19.6	2.5	33 ± 2	0.5
	L258S	7.2 ± 0.3	1.6	213.5 ± 17.9	2.9	34 ± 1	0.5
	L258I	8.8 ± 1.0	2.0	58.4 ± 11.5	0.8	150 ± 10	2.4
	L258H	3.0 ± 0.2	0.7	27.7 ± 3.1	0.4	110 ± 10	1.8
	L258N	15.3 ± 1.3	3.4	196.8 ± 23.5	2.7	78 ± 3	1.3
	L273I	16.4 ± 0.8	3.6	117.0 ± 9.6	1.6	141 ± 8	2.3
	L273V	17.4 ± 0.6	3.9	96.9 ± 10.8	1.3	180 ± 10	2.9
EPS	**WT**	1.2 ± 0.1	1.0	10.9 ± 2.2	1.0	110 ± 20	1.0
	F119Y	3.6 ± 0.1	3.0	14.8 ± 0.5	1.4	240 ± 10	2.2
	F196L	0.5 ± 0.1	0.4	18.9 ± 0.3	1.7	28 ± 3	0.3
	F196I	2.0 ± 0.1	1.7	12.9 ± 1.8	1.2	150 ± 20	1.4
	F196Y	1.9 ± 0.4	1.6	16.5 ± 5.3	1.5	120 ± 10	1.1
	L258S	ND	ND	ND	ND	ND	ND
	L258I	0.7 ± 0.0	0.6	5.1 ± 1.1	0.5	140 ± 30	1.3
	L258H	ND	ND	ND	ND	ND	ND
	L258N	0.1 ± 0.1	0.1	19.1 ± 3.6	1.8	7 ± 2	0.1
	L273I	0.2 ± 0.0	0.2	5.5 ± 1.1	0.5	37 ± 8	0.3
	L273V	0.3 ± 0.0	0.3	10.4 ± 1.4	1.0	29 ± 4	0.3
EPO	**WT**	0.3 ± 0.0	1.0	49.4 ± 9.4	1.0	6 ± 1	1.0
	F119Y	0.8 ± 0.1	2.7	84.4 ± 6.1	1.7	9 ± 0	1.5
	F196L	0.7 ± 0.0	2.3	96.7 ± 5.3	2.0	7 ± 0	1.2
	F196I	1.4 ± 0.1	4.7	130.5 ± 16.4	2.6	11 ± 1	1.8
	F196Y	0.7 ± 0.1	2.3	87.2 ± 18.1	1.8	9 ± 1	1.5
	L258S	0.6 ± 0.1	2.0	74.2 ± 6.3	1.5	8 ± 1	1.3
	L258I	0.5 ± 0.1	1.7	18.7 ± 1.4	0.4	25 ± 2	4.2
	L258H	0.7 ± 0.1	2.3	18.7 ± 3.0	0.4	40 ± 6	6.7
	L258N	1.7 ± 0.1	5.7	102.9 ± 14.7	2.1	17 ± 1	2.8
	L273I	0.7 ± 0.0	2.3	46.7 ± 2.0	0.9	15 ± 1	2.5
	L273V	0.7 ± 0.0	2.3	27.5 ± 3.9	0.6	26 ± 4	4.3
MCO	**WT**	6.9 ± 0.1	1.0	21.4 ± 0.2	1.0	323 ± 7	1.0
	F119Y	3.3 ± 0.3	0.5	52.4 ± 11.3	2.4	65 ± 9	0.2
	F196L	0.5 ± 0.1	0.1	48.5 ± 6.4	2.3	11 ± 1	0.0
	F196I	1.5 ± 0.1	0.2	58.0 ± 6.2	2.7	27 ± 2	0.1
	F196Y	9.5 ± 0.7	1.4	72.7 ± 10.7	3.4	130 ± 10	0.4
	L258S	76.2 ± 2.7	11.0	31.7 ± 4.0	1.5	2410 ± 160	7.5
	L258I	7.0 ± 0.3	1.0	43.0 ± 2.1	2.0	160 ± 20	0.5
	L258H	22.4 ± 1.7	3.2	62.8 ± 8.3	2.9	360 ± 20	1.1
	L258N	133.1 ± 5.9	19.3	35.6 ± 2.3	1.7	3750 ± 240	11.6
	L273I	13.6 ± 0.3	2.0	31.8 ± 4.0	1.5	430 ± 50	1.3
	L273V	17.2 ± 0.6	2.5	20.7 ± 2.7	1.0	840 ± 90	2.6
ECO	**WT**	0.3 ± 0.0	1.0	15.8 ± 4.7	1.0	20 ± 7	1.0
	F119Y	0.3 ± 0.0	1.0	23.3 ± 0.9	1.5	13 ± 3	0.7
	F196L	0.2 ± 0.0	0.7	33.3 ± 4.4	2.1	6 ± 1	0.3
	F196I	0.6 ± 0.0	2.0	33.8 ± 2.5	2.1	18 ± 1	0.9
	F196Y	0.5 ± 0.1	1.7	31.9 ± 4.8	2.0	17 ± 1	0.9
	L258S	10.0 ± 0.2	33.3	12.1 ± 1.2	0.8	830 ± 80	41.5
	L258I	0.4 ± 0.0	1.3	12.6 ± 1.4	0.8	32 ± 4	1.6
	L258H	1.7 ± 0.1	5.7	11.8 ± 1.6	0.7	140 ± 20	7.0
	L258N	27.4 ± 0.7	91.3	24.3 ± 2.1	1.5	1130 ± 70	56.5
	L273I	0.5 ± 0.1	1.7	18.6 ± 2.7	1.2	27 ± 4	1.4
	L273V	0.3 ± 0.0	1.0	8.5 ± 1.8	0.5	36 ± 8	1.8

B

OPs	Variant	k_{cat} (s^{-1})			Relative k_{cat}	Km (μM)			Relative K_m	k_{cat}/K_m (s^{-1} mM^{-1})			Relative k_{cat}/K_m
MPS	**WT**	27.5	±	0.2	1.0	27.3	±	1.4	1.0	1010	±	50	1.0
	R1A6	5.8	±	0.2	0.2	19.1	±	1.7	0.7	310	±	20	0.3
	R1B6	0.3	±	0.0	0.0	19.3	±	4.2	0.7	16	±	4	0.0
	R2B2	0.7	±	0.0	0.0	16.8	±	2.7	0.6	43	±	7	0.0
	R2C2	1.1	±	0.1	0.0	10.6	±	2.8	0.4	110	±	20	0.1
	R2D2	14.1	±	0.5	0.5	10.7	±	1.3	0.4	1320	±	120	1.3
	R2A2	2.3	±	0.2	0.1	28.0	±	4.3	1.0	82	±	6	0.1
	R2F3	1.4	±	0.0	0.1	49.3	±	2.4	1.8	29	±	1	0.0
	R2D4	1.9	±	0.1	0.1	12.1	±	2.4	0.4	160	±	30	0.2
MPO	**WT**	4.5	±	0.2	1.0	72.8	±	6.7	1.0	62	±	3	1.0
	R1A6	37.1	±	1.5	8.2	296.0	±	22.1	4.1	125	±	5	2.0
	R1B6	2.6	±	0.2	0.6	199.4	±	19.3	2.7	13	±	1	0.2
	R2B2	19.7	±	2.3	4.4	326.2	±	49.2	4.5	61	±	3	1.0
	R2C2	3.7	±	0.3	0.8	168.7	±	14.4	2.3	22	±	1	0.4
	R2D2	24.6	±	2.8	5.5	44.8	±	10.2	0.6	560	±	70	9.0
	R2A2	6.8	±	0.6	1.5	173.3	±	20.4	2.4	40	±	2	0.6
	R2F3	6.3	±	0.2	1.4	57.6	±	3.9	0.8	110	±	4	1.8
	R2D4	4.2	±	0.3	0.9	60.2	±	7.9	0.8	70	±	9	1.1
EPS	**WT**	1.2	±	0.1	1.0	10.9	±	2.2	1.0	110	±	20	1.0
	R1A6	1.6	±	0.2	1.3	34.5	±	4.8	3.2	46	±	2	0.4
	R1B6	0.3	±	0.0	0.3	12.8	±	3.2	1.2	25	±	7	0.2
	R2B2	ND			ND	ND			ND	ND			ND
	R2C2	ND			ND	ND			ND	ND			ND
	R2D2	2.3	±	0.2	1.9	25.5	±	3.1	2.3	89	±	5	0.8
	R2A2	2.1	±	0.1	1.8	2.7	±	0.6	0.2	800	±	160	7.3
	R2F3	ND			ND	ND			ND	ND			ND
	R2D4	ND			ND	ND			ND	ND			ND
EPO	**WT**	0.3	±	0.0	1.0	49.4	±	9.4	1.0	6	±	1	1.0
	R1A6	4.4	±	0.2	14.7	46.6	±	2.4	0.9	95	±	3	15.8
	R1B6	7.5	±	0.9	25.0	204.6	±	35.0	4.1	37	±	3	6.2
	R2B2	14.5	±	0.5	48.3	68.8	±	7.4	1.4	210	±	20	35.0
	R2C2	3.3	±	0.3	11.0	31.5	±	3.4	0.6	105	±	5	17.5
	R2D2	11.2	±	0.3	37.3	36.7	±	1.6	0.7	305	±	9	50.8
	R2A2	9.2	±	0.2	30.7	43.8	±	5.4	0.9	210	±	30	35.0
	R2F3	22.0	±	0.7	73.3	37.0	±	2.7	0.7	600	±	20	100.0
	R2D4	13.6	±	0.6	45.3	55.1	±	4.4	1.1	250	±	10	41.7
MCO	**WT**	6.9	±	0.1	1.0	21.4	±	0.2	1.0	323	±	7	1.0
	R1A6	249.2	±	11.4	36.1	17.0	±	3.3	0.8	14930	±	2330	46.2
	R1B6	144.3	±	5.7	20.9	135.5	±	6.7	6.3	1070	±	50	3.3
	R2B2	60.3	±	4.7	8.7	70.4	±	6.4	3.3	860	±	10	2.7
	R2C2	9.8	±	0.2	1.4	56.0	±	2.4	2.6	175	±	5	0.5
	R2D2	118.2	±	7.7	17.1	67.5	±	11.4	3.2	1770	±	160	5.5
	R2A2	3.9	±	0.1	0.6	70.6	±	2.8	3.3	55	±	1	0.2
	R2F3	42.5	±	3.3	6.2	104.5	±	14.4	4.9	410	±	25	1.3
	R2D4	10.4	±	0.2	1.5	57.2	±	2.8	2.7	183	±	6	0.6
ECO	**WT**	0.3	±	0.0	1.0	15.8	±	4.7	1.0	20	±	7	1.0
	R1A6	91.3	±	3.3	304.3	17.8	±	0.6	1.1	5120	±	40	256.0
	R1B6	109.8	±	2.0	366.0	50.2	±	4.6	3.2	2200	±	220	110.0
	R2B2	30.9	±	1.3	103.0	13.6	±	2.8	0.9	2270	±	80	113.5
	R2C2	4.3	±	0.1	14.3	14.5	±	0.6	0.9	290	±	10	14.5
	R2D2	33.5	±	0.5	111.7	43.6	±	4.3	2.8	770	±	70	38.5
	R2A2	2.8	±	0.1	9.3	21.7	±	5.8	1.4	130	±	20	6.5
	R2F3	36.4	±	2.7	121.3	23.4	±	3.6	1.5	1570	±	150	78.5
	R2D4	10.2	±	0.3	34.0	18.7	±	1.9	1.2	550	±	50	27.5

R1A6	F119Y, L258S
R1B6	F196I, L258N
R2B2	F196I, L258H
R2C2	F196I, L273I
R2D2	F119Y, L258H
R2A2	F119Y, F196I, L273V
R2F3	F119Y, F196Y, L258H
R2D4	F119Y, F196I, L273I

Only 35% of the library has an activity that is less than 50% of that of the wild-type enzyme (Fig. S1 in the Supplemental material). L258 forms part of the base of the active site pocket in MPH. The beneficial mutations are largely hydrophilic (L258H, L258N and L258S; the L258I leads to some modest improvements in catalytic efficiency). The effect of the L258S and L258N mutations is similar: both variants display an increase in k_{cat} for oxon OPs but a decrease for thiolphosphate OPs (Table 3A). Both variants also show a large increase in k_{cat} for chlorpyrifos-based OPs (*i.e.* MCO and ECO); L258S is 11-fold and 32-fold more reactive towards MCO and ECO, respectively. The corresponding increase in activity for the L258N mutant is 19-fold and 91-fold. The increase in k_{cat} is also

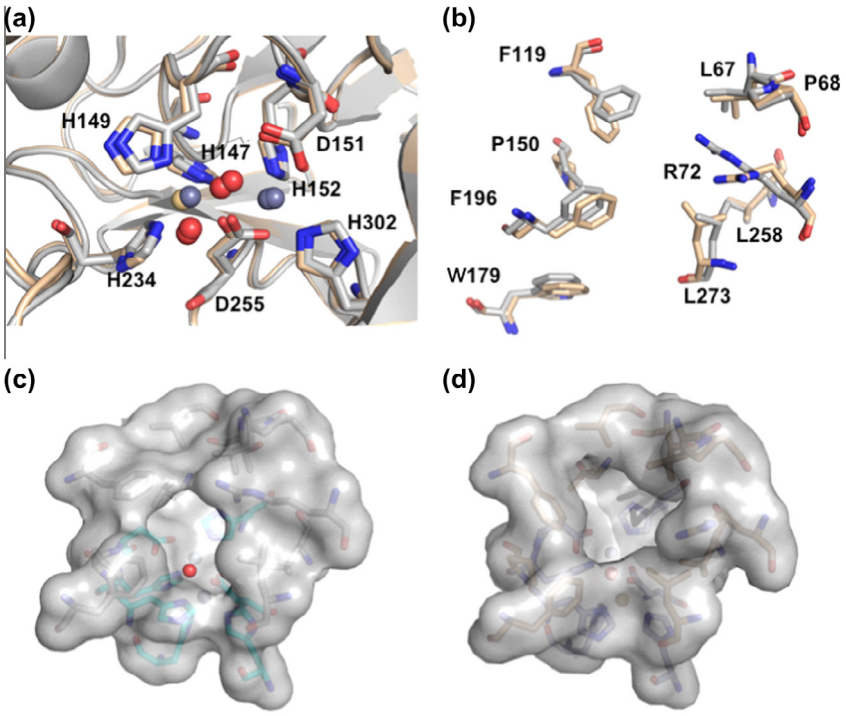

Fig. 5. Active site conformations of the two MPH monomeric subunits. The metal ion center superimposition of the two MPH subunits is shown in (a). The superimposition of active site-lining residues is shown in (b). The active site-lining residues for subunit A are shown in (c) and those for subunit B in (d). The surface represents the solvent-excluded surface of the active site.

reflected in an enhancement of the catalytic efficiency (k_{cat}/K_m) of L258S and L258N towards these substrates to an extent that they are more efficient than wild-type MPH towards MPS, its optimal substrate (see Introduction). The k_{cat}/K_m values towards MCO and ECO are $2.42 \times 10^6\ s^{-1}\ M^{-1}$ and $0.96 \times 10^6\ s^{-1}\ M^{-1}$, and $3.73 \times 10^6\ s^{-1}\ M^{-1}$ and $1.13 \times 10^6\ s^{-1}\ M^{-1}$ for L258S and L258N MPH, respectively. Although the reasons for these considerable improvements are currently unknown the increased hydrophilicity in the active sites of the mutants may provide the basis for a more efficient mode of substrate binding. While the L258H mutation also leads to some (minor) improvement in catalytic efficiency towards MCO and ECO (Table 3A) its main effect is a sixfold increase in the catalytic efficiency towards EPO. In contrast, the L258R mutation is detrimental for the catalytic efficiency of MPH, likely to be due to the large size of this side chain.

L273 mutations – conservative but beneficial

L273I and L273V are mutations that lead to an improvement in the catalytic efficiency of MPH towards EPO (Table 3A). L273I and L273V mutations are conservative mutations and probably represent the rearrangement of side chains to allow better access to substrates. This interpretation is in agreement with an earlier study on MPH where the L273A mutation was shown to have a similar catalytic effect [13]. For both L273I and L273V, an increase in k_{cat}/K_m for all oxon substrates is observed, while the catalytic efficiency towards MPS and EPS is reduced by these mutations. Since L258 and L273 are located near each other and mutations to these sites improve the catalytic efficiencies towards oxon substrates, it is likely that this part of the substrate-binding pocket determines the specificity in favor of oxonate rather than thionate substrates. It is worth noting, however, that although L273 mutations lead to an increase in efficiency towards oxonate substrates and a significant decrease towards thionates, the measured catalytic efficiencies for thionates are still higher than those for their oxonate analogues.

L67, P68, R72, P150 and W179 are sites intolerant to mutations

The roles of L67, P68 and R72 are unclear at this point. However, activity distributions of L67P68R72 NDT and R72 NNK libraries suggest that these sites are intolerant towards mutations. For both libraries, more than 80% of mutants screened have shown less than 50% of the EPO activity measured for wild-type MPH and no variants with improved catalytic efficiency were found (Fig. 3A). For R72, mutations R72A, R72T and R72G resulted in relative activities of 36%, 14% and 11% respectively, suggesting an important role in either catalysis or substrate binding or both. The crystal structure of wild-type MPH (PDB ID: 1P9E) does not indicate relevant interactions R72 may be involved in. However, a closer comparison of the active sites of the two subunits in the homodimer reveals conformational differences in some of the residues, particularly R72, F119 and L273 (Fig. 5). Judged from the *B*-factors extracted from the crystal structure these residues are located in a flexible region. Furthermore, docking studies with the two subunits of MPH and the substrate MPS (using SwissDock [32,33] and AutoDock Vina [31]) indicate that the conformation observed in subunit B is the form adopted by the enzyme during catalysis as MPS can only be successfully docked into this subunit (Fig. S3 in the Supplemental material). This also suggests that the conformation observed in subunit A restricts substrate access and thus impedes catalysis.

In the P150 NDT library, the P150Y and P150H mutations were found to result in a large drop in activity, with the mutants having only 27% and 8%, respectively, of the activity of wild-type MPH. This is likely to be due to the steric obstruction introduced by the relatively large side chains of tyrosine and histidine. P150 is surrounded by L118, F119 and F196. Mutating P150 into residues with larger side chain will thus introduce clashes with aforementioned residues, especially F119 and F196, causing a loss in activity.

In the W179 NNK library, W179S, W179H, W179Y and W179M were the deleterious mutations sampled. The deterioration in activity may be due to the disruption of hydrogen bonding between W179 and E175. E175 appears to act as a bridging residue

Table 4
Comparison of the catalytic efficiencies of wild-type and selected MPH mutants towards a range of substrates. ND: Not determined.

Substrates	k_{cat}/K_m (s^{-1} M^{-1})			
	WT	R1A6	R2F3	R2D2
MPS	1.0×10^6	3.1×10^5	2.9×10^4	1.3×10^6
MPO	6.2×10^4	6.2×10^3	1.3×10^5	5.6×10^5
EPS	1.1×10^5	4.6×10^4	ND	8.9×10^4
EPO	6.2×10^3	9.5×10^4	6.0×10^5	3.1×10^5
MCO	3.2×10^5	1.5×10^7	4.1×10^5	1.8×10^6
ECO	2.0×10^4	5.1×10^6	1.6×10^6	7.7×10^5

between the side chain of W179 and the backbone of M148, suggesting a structural role for W179. However, Dong et al. found that the mutation W179F retains catalytic parameters (k_{cat} and K_m) similar to those of wild-type MPH, suggesting that the interaction between W179 and E175 is not important and any aromatic side chain may replace W179 for effective substrate binding [10].

Multiple site mutants obtained from shuffling show interesting profiles

The mutant R1A6 (F119Y, L258S) displays improvements for all substrates examined except MPS, the preferred substrate for wild-type MPH (Table 3B). The improvements in k_{cat} and k_{cat}/K_m towards the hydrolysis of EPO, the OP used for screening, are approximately 15-fold. However, the largest improvement observed for this mutant was towards MCO and ECO; for MCO k_{cat} and k_{cat}/K_m improved 36- and 46-fold, respectively, and for ECO the corresponding increases were 304- and 252-fold. The catalytic efficiencies of the mutant for MCO and ECO, respectively, are thus ~15-fold (1.47×10^7 s^{-1} M^{-1}) and ~fivefold (5.13×10^6 s^{-1} M^{-1}) larger than that of wild-type MPH for MPS (1.01×10^6 s^{-1} M^{-1}). The kinetics data obtained for R1A6 are also consistent with the observation that the L258S mutation introduces a preference for chlorpyrifos-type substrates (*vide infra*).

The R2F3 mutant (F119Y, F196I, L258H) is the most efficient mutant towards EPO (Table 3B). The mutant has an over 73-fold increased k_{cat} and nearly 100-fold improvement of k_{cat}/K_m for EPO when compared to wild-type MPH. This mutant also has ~121-fold and 77-fold improvements in k_{cat} and k_{cat}/K_m, respectively, for the reaction with ECO, thus making it a very efficient catalyst for the hydrolysis of diethyl oxon substrates.

The R2D2 mutant (F119Y, L258H) is a 'generalist', with k_{cat} improvements for all substrates except MPS (Table 3B). While the k_{cat} for MPS has decreased, the k_{cat}/K_m is similar to that of wild-type MPH (due to a decrease in K_m). Of the six substrates examined, five have k_{cat}/K_m values of at least 1×10^5 s^{-1} M^{-1}; two of these five are at least 1×10^6 s^{-1} M^{-1}, representing a significant improvement compared to wild-type MPH (Table 4); this variant is thus a good candidate for application in bioremediation. A comparison of the catalytic efficiencies of R1A6, R2F3 and R2D2 with that of wild type MPH is summarized in Table 4.

Concluding remarks

The work presented here describes a site saturation mutagenesis study of residues lining the active site of MPH and the directed evolution of this enzyme for improved EPO hydrolysis. To the best of our knowledge, this is the most extensive substrate profile characterization of MPH and related OP-degrading enzymes to date and provides essential clues about the development of specific mutants useful for bioremedial applications. The substrate profiles of single site mutants were characterized with various OP substrates in an attempt to understand the roles of these residues in substrate interaction(s). All the selected single site mutants have modest improvements for EPO hydrolysis and, interestingly, unexpected but impressive improvements were observed for L258 mutants for the hydrolysis of non-selected substrates (MCO and ECO). Subsequently, two rounds of directed evolution were conducted with the aim to further enhance the EPO-hydrolyzing

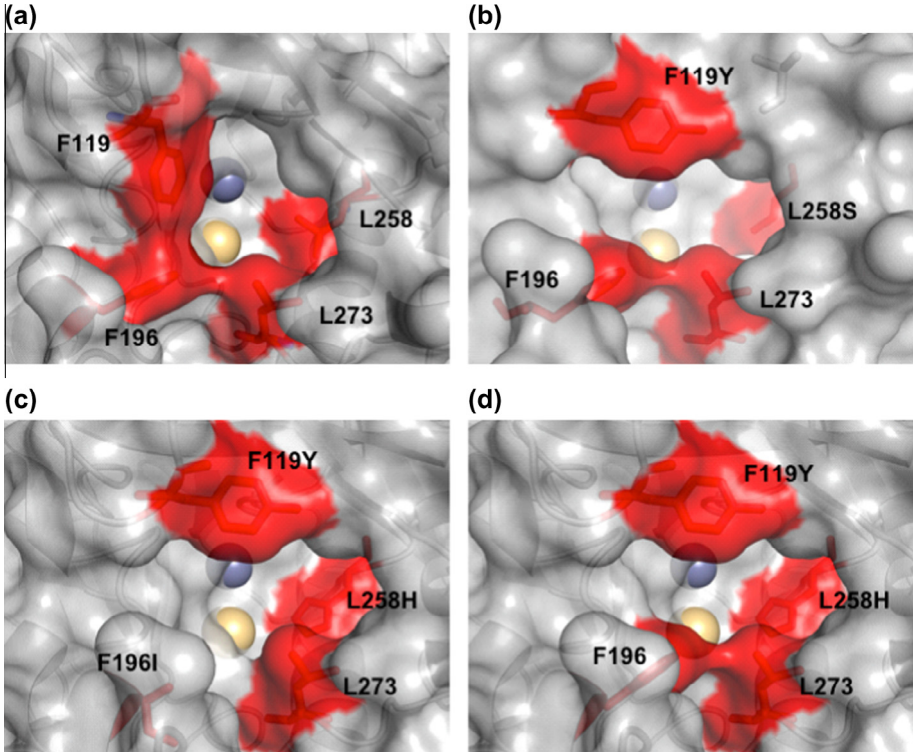

Fig. 6. Comparison of the active site pockets of selected MPH variants and the wild-type enzyme. (a) wild-type MPH, (b) R1A6 mutant, (c) R2F3 mutant, and (d) R2D2 mutant.

efficiency of MPH; numerous multiple site mutants with improved activity were obtained. These results highlight the robustness and 'plasticity' of the MPH active site to accommodate and turn over different OP substrates – a few amino acid changes in the active site pocket result in drastic changes in OP specificity. Most of the beneficial mutations observed can be attributed to changes in the shape of active site pocket, as shown by MPH mutants modelled with SWISS-MODEL (Fig. 6). Thus, in summary, the ease of altering its substrate specificity make MPH a strong candidate for bioremediation and pharmaceutical applications.

Acknowledgments

This work was financially supported by the Australian Research Council, Discovery Projects Scheme (DP120104263). T.-K.N. is supported by an Australian National University PhD Scholarship and an Australian National University Research Scholarship. G.S. also acknowledges the receipt of an ARC Future Fellowship (FT120100694).

Appendix A. Supplementary data

Supplementary data associated with this article can be found, in the online version, at http://dx.doi.org/10.1016/j.abb.2015.03.012.

References

[1] POST (1998) Organophosphates. Parliamentary Office of Science and Technology, 122.
[2] F. Ely, J.-L. Foo, C.J. Jackson, L.R. Gahan, D.L. Ollis, G. Schenk, Curr. Top. Biochem. Res. 9 (2007) 63–78.
[3] J. Jeyaratnam, World Health Stat. Q. 43 (1990) 139–144.
[4] I.B. Wilson, Ann. N. Y. Acad. Sci. 135 (1966) 177–183.
[5] I.B. Wilson, S. Ginsburg, Biochim. Biophys. Acta 18 (1955) 168–170.
[6] A.A. Weinbroum, Br. Med. Bull. 72 (2004) 119–133.
[7] F. Worek, H. Thiermann, L. Szinicz, P. Eyer, Biochem. Pharmacol. 68 (2004) 2237–2248.
[8] A. Ekkhunnatham, B. Jongsareejit, W. Yamkunthong, J. Wichitwechkarn, World J. Microb. Biot. 28 (2012) 1739–1746.
[9] R. Zhang, Z. Cui, X. Zhang, J. Jiang, J.-D. Gu, S. Li, Biodegradation 17 (2006) 465–472.
[10] Y.-J. Dong, M. Bartlam, L. Sun, Y.-F. Zhou, Z.-P. Zhang, C.-G. Zhang, Z. Rao, X.-E. Zhang, J. Mol. Biol. 353 (2005) 655–663.
[11] A.F. Neuwald, J.S. Liu, D.J. Lipman, C.E. Lawrence, Nucleic Acids Res. 25 (1997) 1665–1677.
[12] H. Daiyasu, K. Osaka, Y. Ishino, H. Toh, FEBS Lett. 503 (2001) 1–6.
[13] Y.-S. Jeong, S.-L. Choi, H.-H. Kyeong, J.-H. Kim, E.-J. Kim, J.-G. Pan, E. Rha, J.J. Song, S.-G. Lee, H.-S. Kim, Des. Sel. 25 (2012) 725–731.
[14] J. Liu, Y. Boucher, H.W. Stokes, D.L. Ollis, Protein Exp. Purif. 47 (2006) 258–263.
[15] H.-K.S. Leiros, P.S. Borra, B.O. Brandsdal, K.S.W. Edvardsen, J. Spencer, T.R. Walsh, O. Samuelsen, Antimicrob. Agents Chemother. 56 (2012) 4341–4353.
[16] A. Carfi, E. Duée, M. Galleni, J.M. Frère, O. Dideberg, Sect. D: Biol. Crystallogr. D54 (1998) 313–323.
[17] G. Garau, C. Bebrone, C. Anne, M. Galleni, J.-M. Frère, O. Dideberg, J. Mol. Biol. 345 (2005) 785–795.
[18] J.H. Ullah, T.R. Walsh, I.A. Taylor, D.C. Emery, C.S. Verma, S.J. Gamblin, J. Spencer, J. Mol. Biol. 284 (1998) 125–136.
[19] A.D. Cameron, M. Ridderström, B. Olin, B. Mannervik, Structure 7 (1999) 1067–1078.
[20] V.A. Campos-Bermudez, N.R. Leite, R. Krog, A.J. Costa-Filho, F.C. Soncini, G. Oliva, A.J. Vila, Biochemistry 46 (2007) 11069–11079.
[21] M.H. Kim, W.-C. Choi, H.O. Kang, J.S. Lee, B.S. Kang, K.-J. Kim, Z.S. Derewenda, T.-K. Oh, C.H. Lee, J.-K. Lee, Proc. Natl. Acad. Sci. U.S.A. 102 (2005) 17606–17611.
[22] B. Kostelecky, E. Pohl, A. Vogel, O. Schilling, W. Meyer-klaucke, J. Bacteriol. 188 (2006) 1607–1614.
[23] W.-C. Tseng, J.-W. Lin, T.-Y. Wei, T.-Y. Fang, Anal. Biochem. 375 (2008) 376–378.
[24] J. Sanchis, L. Fernández, J.D. Carballeira, J. Drone, Y. Gumulya, H. Höbenreich, D. Kahakeaw, S. Kille, R. Lohmer, J.J.-P. Peyralans, J. Podtetenieff, S. Prasad, P. Soni, A. Taglieber, S. Wu, F.E. Zilly, M.T. Reetz, Appl. Microbiol. Biotechnol. 81 (2008) 387–397.
[25] H. Zhao, L. Giver, Z. Shao, J.A. Affholter, F.H. Arnold, Nat. Biotechnol. 16 (1998) 258–261.
[26] B.J. Stevenson, J.-W. Liu, D.L. Ollis, Biochemistry 47 (2008) 3013–3025.
[27] G. Fu, Z. Cui, T. Huang, S. Li, Protein Exp. Purif. 36 (2004) 170–176.
[28] N. Guex, M.C. Peitsch, Electrophoresis 18 (1997) 2714–2723.
[29] T. Schwede, J. Kopp, N. Guex, M. Peitsch, Nucleic Acids Res. 31 (2003) 3381–3385.
[30] K. Arnold, L. Bordoli, J. Kopp, T. Schwede, Bioinformatics 22 (2006) 195–201.
[31] O. Trott, A.J. Olson, J. Comput. Chem. 31 (2010) 455–461.
[32] A. Grosdidier, V. Zoete, O. Michielin, J. Comput. Chem. 32 (2011) 2149–2159.
[33] A. Grosdidier, V. Zoete, O. Michielin, Nucleic Acids Res. 39 (2011) W270–W277.
[34] H. Yang, P.D. Carr, S.Y. McLoughlin, J.W. Liu, I. Horne, X. Qiu, C.M.J. Jeffries, R.J. Russell, J.G. Oakeshott, D.L. Ollis, Protein Eng. 16 (2003) 135–145.
[35] M.T. Reetz, D. Kahakeaw, R. Lohmer, ChemBioChem 9 (2008) 1797–1804.
[36] H. Zhao, W. Zha, Nat. Protoc. 1 (2006) 1865–1871.
[37] G. Gotthard, J. Hiblot, D. Gonzalez, M. Elias, E. Chabriere, PLoS One 8 (2013) e77995.